

# Autonomous Integrity

## An Error Isotropy–Based Approach for Multiple Fault Conditions

MIGUEL AZAOLA-SÁENZ AND JOAQUÍN COSMEN-SCHORTMANN, GMV

Copyright iStockphoto.com/Alexander von Sydow

Within the great effort being spent on improving GNSS integrity-assurance techniques in order to achieve higher service levels for civil aviation, special attention is being paid to user-based solutions, as reflected in the conclusions of the Federal Aviation Administration’s GNSS Evolutionary Architecture Study (GEAS) panel. This article introduces an autonomous technique for computing protection levels based on error isotropy that, unlike conventional methods, adapts in real-time to ranging error size and also handles multiple-fault conditions.

In trying to ensure integrity of GNSS navigation systems for civil aviation, various approaches have produced a range of different concepts, most of which assume the computation of a protection level. This computation is usually accomplished either autonomously (that is, entirely based on information gathered by the user receiver) or with some degree of external assistance.

Such information may be provided by integrity augmentation systems (for example, space-based or ground-based augmentation systems — SBAS and GBAS). It may also be provided directly by the GNSS constellation, as it is foreseen with the future GPS III — remarkably enough, the GPS SPS Performance Standard already includes integrity per-

formance specifications — and Galileo.

Autonomous protection-level computation techniques, however, have never been seriously considered as reliable sole means for ensuring integrity in safety-of-life (SoL) applications, not only because of the poor performances achieved, but also due to the somewhat delicate assumptions all of them rely upon. As a result, such techniques have mostly been considered as complementary to external integrity systems. One example: GPS+receiver autonomous integrity monitoring (RAIM) is not allowed as a primary navigation means for precision approach operations.

Recently, in regard of the improvements on accuracy and reliability expected from the future constellations

GPS III and Galileo, new approaches have been proposed for the apportionment of integrity requirements. This is reflected, for instance, in the conclusions presented in the Phase I report of the USA *GNSS Evolutionary Architecture Study* (GEAS). The report suggests that the allocation of the burden for providing integrity should be balanced towards the user receiver, thus conferring user-based integrity (that is, receiver autonomous integrity) a higher responsibility.

User-based integrity is also gaining importance due to the emergence of a new field of GNSS applications, the so called *liability-critical applications* (i.e., those where undetected GNSS large position errors can generate significant legal or economic negative conse-

quences). Some leading examples of such applications are road tolling/congestion charging (both for highways and city areas), law enforcement (e.g., speed fining or surveillance of parolees) or “pay as you drive” insurance schemes.

## IBPL simplifies the interoperation of multiple GNSS constellations for integrity purposes, avoiding the problem of combining different integrity concepts

Unlike air navigation, liability-critical applications often take place in harsh operating environments dominated by local effects such as multipath. Under such conditions these applications cannot always be monitored or aided by external (global, regional, or even local) augmentation systems.

Even in civil aviation, some landing operations could also be subject to large multipath that could put the navigation integrity at risk. For those scenarios the proposed technology would mitigate the associated risk.

One key assumption of conventional RAIM schemes is that simultaneous faulty measurements are extremely unlikely. This single-fault assumption, however, fails to hold in a typical liability-critical application scenario, where multipath is the primary source for large measurement errors and will quite frequently affect more than one measurement at a time. The single-fault assumption also fails to hold in the future air navigation scenario, where the large number of satellites made available by the joint use of several constellations (GPS/Galileo/GLONASS) will significantly increase the probability of multiple simultaneous faults.

Other assumptions common to all existing RAIM schemes include one or another statistical model of the individual measurement errors, trying in particular to bound the tails of their distributions. This sort of assumption is somewhat risky and difficult to verify, especially when the target confidence level is very high, as in the case of SoL applications such as civil aviation.

Moreover, under heavy multipath conditions most statistical assumptions

of this nature just do not hold as errors caused by multipath are strongly dependent on the geometric characteristics of the local environment. (An especially acute example of this is non-line-of-sight (NLoS) multipath — that is, when

a signal is tracked by GNSS equipment as it reflects from some surface despite the fact that a direct view of the satellite is occluded by some obstacle.) Hence, it is almost impossible to come up with a statistical characterization of such errors that can be used for integrity monitoring.

In this article we present a novel technique for autonomous computation of protection levels, the *isotropy-based protection level* concept, or IBPL

for short. This technique makes no particular assumption on the statistics of individual measurement errors and provides coverage against multiple fault conditions. It takes advantage of a possible future multi-constellation scheme as its performance improves rapidly with the amount of satellites used for positioning.

Discussion in this article will show that asymptotic performance of the IBPL with respect to the number of satellites is comparable to that obtained with SBAS protection levels. This fact makes the IBPL a very promising technique, not only for liability-critical applications (the framework where it was born) but also, and very particularly, for SoL applications. We believe that IBPL fits remarkably well in the scheme proposed by the GEAS panel mentioned earlier, which recommends a shift of the integrity responsibility towards the on-board equipment.

**TURN TO PCTEL FOR APPLICATION-FOCUSED GPS/SATCOM ANTENNA SOLUTIONS**

PCTEL designs and manufactures high performance antennas to provide precise operation, maximum durability, and ease of installation for applications in:

- Network Timing
- Vehicle/Asset Tracking
- Public Safety
- Military
- Satellite Communications
- Aviation
- Precision Measurement
  - Agriculture
  - Construction

*For your custom, application-specific, GPS/SATCOM antenna designs contact the PCTEL sales team.*

**A LEADING PROVIDER OF HIGH PERFORMANCE GPS/SATCOM ANTENNAS**

**PCTEL™**  
simplifying mobility

phone 630.372.6800  
toll-free 800.323.9122  
website antenna.pctel.com  
email sales.antenna@pctel.com

Furthermore, as a fully autonomous method, the IBPL-based approach does not require integrity information to be transmitted on the GNSS or SBAS signal in space. This dramatically simplifies the interoperation of multiple GNSS constellations for integrity purposes, avoiding the problem of combining different integrity concepts from the various constellations or augmentation systems.

### Autonomous Integrity: Two Approaches

For liability-critical applications, particularly in urban areas, local effects such as multipath — especially NLoS multipath — are by far the main source of errors and, consequently, the main threat to accuracy and integrity. In this

#### The IBPL algorithm does not implement measurement rejection techniques but rather computes a protection level based on the all-in-view least squares solution.

framework, the conventional notion of faulty measurement as a large measurement error caused by a satellite malfunction is no longer useful.

Instead, a large measurement error is much more likely to be caused by some local effect (primarily NLoS multipath) than by a system failure of any kind. Furthermore, large errors caused by local effects can be so common that any efficient detection and exclusion algorithm would frequently reject too many observations to allow navigation. This is why we need to consider other approaches to the integrity problem, at least for harsh environments.

On one hand, as we have just explained, the traditional concept of achieving integrity operates on the principle of rejecting “faulty” measurements. This is what we will call the *measurement rejection approach* (MRA), which works well in open-sky environments. Focusing on integrity and disregarding its potentially reduced availability, MRA can also work in other environments as long as the detection/exclusion algorithms used do not assume that only a single fault can occur at one time, and

removal of such assumption is itself a serious challenge.

Another approach is to characterize measurement errors and be able to compute a protection level that protects against them, without the need for identifying and removing degraded measurements, even if they are contaminated with very large errors. This is the *error characterization approach* (ECA). In an ECA implementation, as soon as measurement errors increase or decrease, so does the computed protection level. No matter how large the error of a measurement is, that measurement will be used for navigation, but the computed protection level has to account for it so as to keep bounding user position error.

Both approaches can lead to the same level of integrity, the trade-off

being a matter of protection level sizes and their associated availability. Service availability, understood as the probability that the navigation system is usable for a particular application at a particular time, requires that:

- A navigation solution exists with an associated protection level.
- The protection level is small enough to suit the requirements of the particular application.

The first requirement conflicts with the MRA, whereas the second one conflicts with the ECA.

In open-sky environments, where local effects are rare and small, both the MRA and the ECA can yield quite the same availability performance. However, in harsh environments, the MRA alone is clearly insufficient, and that is why the authors developed the ECA concept and the IBPL as the key for a successful ECA implementation.

However, when the authors looked back to the open-sky environments in which both approaches are expected to work almost as well, the IBPL proved to be such a powerful technique as to suggest its use for SoL applications (of which

civil aviation is probably the clearest exponent).

### IBPL: the Concept

The IBPL algorithm does not implement measurement rejection techniques but rather computes a protection level based on the all-in-view least squares solution. Of course, other IBPL solutions are possible, for instance, when different subsets of measurements are used and the one with smallest IBPL is selected. However, in its simplest form (as described in this article), this algorithm is a strict ECA concept implementation. On the other hand, this does not exclude the possibility that some refinements can be made for open-sky applications by including some kind of fault detection/exclusion mechanism.

The idea for the basic IBPL algorithm is to use the vector of least squares estimation residuals (or the *residual vector*) as a characterization of the position error: the larger the residual vector, the larger the state estimation error vector (from a statistical perspective). The relation between both is taken to be linear; so, the protection level depends linearly on the size of the residual vector.

Of course, the state estimation error also depends on the dilution of precision (DOP); so, if we are interested in a horizontal protection level (a vertical protection level would be obtained analogously), we would compute it as:

$$HPL = k \cdot \|r\| \cdot HDOP$$

where  $r$  is the least squares residual vector and  $k$  is the proportionality constant that relates the residual size with the state estimation error.

This constant  $k$ , which depends on the target confidence level  $1 - \alpha$  of the protection level as well as on the number of measurements used for the estimation, is called the *isotropic confidence ratio* (ICR). It is defined so as to ensure that the state estimation error  $\delta$  (or, more precisely, its image in the measurement space through the observation matrix  $H$ ) is bounded by the size of the residual vector up to the ICR and the target confidence level  $1 - \alpha$ , according to the formula:

$$P(\|H \cdot \delta\| > k \cdot \|r\|) \leq \alpha$$

For computing  $k$  from the preceding relation, we assume that the measurement error vector has an isotropic distribution in the measurement space (and, hence, the name for the constant  $k$ ). That is, the error vector can point in any direction of the measurement space with the same probability. Note that this does not imply any particular distribution of the individual measurement errors (e.g., “Gaussianity”), nor that they are unbiased or have known variance. Individual errors can be arbitrarily large or biased as long as they define an error vector that has the same a priori probability of pointing in any direction of the measurement space.

Notice that, when conventional navigation and RAIM methods assume centered “Gaussianity” and independence of errors, isotropy holds as a trivial consequence; so, isotropy is less a stringent assumption than those taken in conventional techniques.

Isotropy implies that the pointing direction of the error vector defines a uniform distribution in the unit  $N-1$ -dimensional sphere of the  $N$ -dimensional measurement space. On the other hand, the condition  $\|H \cdot \delta\| > k \cdot \|r\|$  is a condition on the ratio between the sizes of the vectors  $H \cdot \delta$  and  $r$ , which happen to be orthogonal in the measurement space. Therefore, the said condition defines a region of the sphere, the area of which depends on  $k$ .

Hence, in order to compute the ICR for a given confidence level  $1 - \alpha$ , it suffices to impose that the area of the region so defined is a  $\alpha$  fraction of the total area of the sphere. Thus, if the whole sphere represents all possible pointing directions for the error vector, and hence has probability 1, the region so obtained represents a set of possible pointing directions with probability  $\alpha$ .

Note that the dimension of the measurement space is equal to the number of measurements; so, we are dealing with a multi-dimensional sphere, and the result depends on the dimension. Hence, the value of the ICR depends on both  $\alpha$  and the number of measurements,  $N$ :

$N \setminus \alpha$	$10^{-1}$	$10^{-2}$	$10^{-3}$	$10^{-4}$	$10^{-5}$	$10^{-6}$	$10^{-7}$
5	14.94	150.0	1500.0	$1.5 \times 10^4$	$1.5 \times 10^5$	$1.5 \times 10^6$	$1.5 \times 10^7$
6	4.30	14.09	44.70	141.42	447.21	1414.21	4472.13
7	2.67	6.19	13.52	29.22	62.98	135.72	292.40
8	2.03	4.00	7.31	13.11	23.37	41.60	74.00
9	1.68	3.02	4.99	8.03	12.80	20.33	32.25
10	1.46	2.47	3.82	5.74	8.51	12.55	18.46
11	1.30	2.12	3.13	4.49	6.32	8.85	12.35
12	1.18	1.87	2.68	3.71	5.04	6.79	9.10
13	1.09	1.69	2.36	3.18	4.20	5.50	7.16
14	1.02	1.56	2.12	2.80	3.62	4.64	5.90
15	0.96	1.44	1.94	2.52	3.20	4.02	5.02

TABLE 1. Example of ICR pre-computed values

$$k = k(\alpha, N)$$

In solving this problem, one comes across multidimensional integral equations that can be numerically solved for a pre-selected set of values of  $\alpha$  and  $N$  and tabulated for faster real time performance. Table 1 presents an example of this. Similar tables can be computed for different navigation modes; for instance, in the case of relative or kinematic navigation, where the clock parameter gets removed from the problem by double-differencing measurements of both the base and the rover receivers, there are only three parameters to estimate, which yields a slightly different table.

Note from Table 1 the high sensitivity of the ICR to the number of measurements. Observe, for instance, that for  $\alpha = 10^{-7}$  the value of  $k$  drops from  $1.5 \cdot 10^7$  to  $4.4 \cdot 10^3$  just by passing from 5 to 6 measurements. This means that when measurement redundancy is low, residuals constitute much less reliable a measure of position errors. (In particular, although not made explicit in Table 1, with four measurements the ICR would grow to infinity, because no finite bound can be guaranteed in the absence of measurement redundancy, regardless of the target confidence level.)

As a consequence, availability performance becomes poor in environments with reduced visibility of the sky, such as urban areas, as the isotropy-based protection level tends to be very large. However, this type of protection level

exhibits a great performance in open-sky areas.

Remarkably, the IBPL concept provides protection against simultaneous multiple faults, because it does not depend on the number of faulty measurements occurring at the same time nor on the sizes of their errors: simultaneous faults combine to produce a certain measurement error, but no a priori privileged directions exist for the measurement error vector to point to; hence, the isotropy assumption is not violated by multiple fault conditions.

### Validating IBPL Integrity

Of course, we need to validate this new protection level concept and its underlying isotropy assumption in terms of the achieved integrity, and that must be done by experimentation with real data. We have to show that the theoretical confidence level of the isotropy-based protection level is satisfied in real life. Our discussion here cannot be considered as a full validation of the IBPL concept, but it provides significant information about the validity of the proposed algorithms.

For that purpose it is very convenient to be able to compute protection levels for various confidence levels — especially for low ones, say, from  $1-10^{-4}$  down to  $1-10^{-1}$  — because much smaller measurement campaigns are required (in order to have a representative statistical sample) than for a high confidence level such as  $1-10^{-7}$  (required for civil aviation applications).

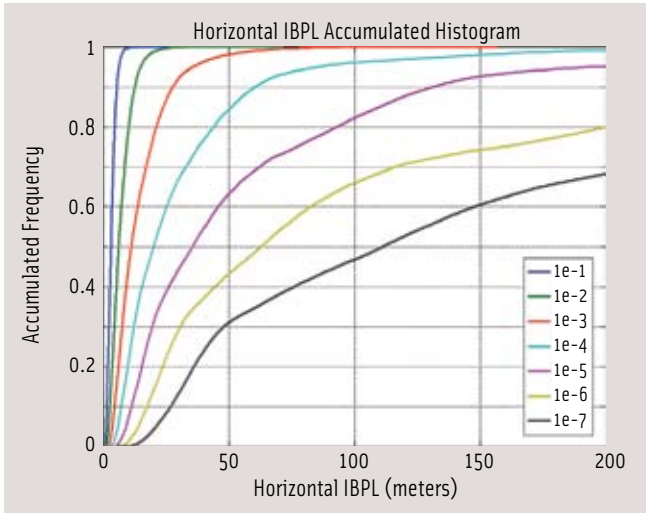


**FIGURE 1** IBPL availability in open sky, GPS only

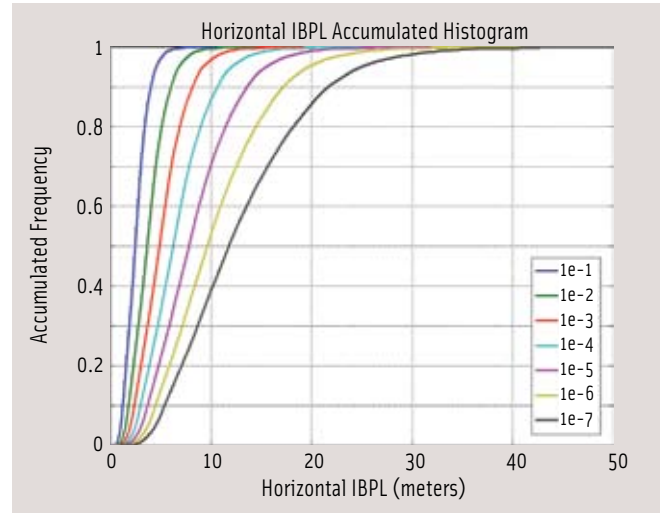


**FIGURE 2** IBPL open sky availability, GPS + GLONASS/Galileo (extrapolation)

$\alpha$	$10^{-1}$	$10^{-2}$	$10^{-3}$	$10^{-4}$
<b>Horizontal MI Rate</b>	0.088	0.0070	0.000417	0
<b>Vertical MI Rate</b>	0.055	0.0036	0.000069	0

**TABLE 2.** Horizontal Misleading Information Results

Experimental validation has been driven based on an open-sky data set 28,800 epochs long of real GPS measurements from December 17, 2007, collected at the International GNSS Service (IGS) station Villafranca, Spain. (Further validation with much larger data sets is foreseen in the near future.) Integrity results are summarized in **Table 2**, which shows the horizontal misleading information (MI) event rates obtained in both scenarios for different values of  $\alpha$ . (An MI event occurs when the protection level is exceeded by the position error.)

As can be seen in Table 2, the MI rates are very close to their theoretical values (given by the corresponding  $\alpha$ ). The reader will notice, however, that these results show some degree of conservativeness. This is due to the fact that DOP is a scalar measure of the ratio of a vector transformation, given by the matrix  $H$ , between the measurement space and the state space and, as such, DOP is conservative.

The definition of the IBPL can be refined to account for this effect in order

to obtain tighter MI rates. Apart from that, these results represent a promising confirmation of the integrity of the method and, therefore, of the validity of its underlying isotropy assumption.

Although demonstrating performance in an urban environment is not the aim of this article, it is worthwhile to mention that parallel tests with urban data have been carried out with similar integrity results, thus confirming the robustness of IBPL against multiple fault conditions.

### IBPL Performance Results

From the same open-sky test run for IBPL integrity validation we derive performance figures in the form of accumulated histograms of protection level sizes. **Figure 1** represents an IBPL accumulated histogram that, for each possible size between 0 and 200 meters, represents the relative frequency at which IBPL has occurred below that size throughout the test. The histogram accounts for 28,800 samples (just as many as the number of measurement epochs) and has different curves, each representing a different confidence level  $1 - \alpha$  from  $1 - 10^{-1}$  up to  $1 - 10^{-7}$ .

Observe that IBPL accumulated histograms constitute a good way to figure out service availability (for whatever type of application the IBPL could be used) as they provide information both on IBPL sizes and on associated frequencies.

Observe also from the figure that IBPL availability is not far from that achieved with conventional RAIM protection-level computation techniques, although IBPL is not relying on the single fault assumption nor on assumed measurement error size statistics. RAIM assumptions on error sizes tend to be conservative to compensate for certain model weaknesses, such as the fact that real-life errors do not follow a Gaussian distribution. This is partially compensated by the single-fault assumption on which RAIM relies; so, at the end they produce quite a similar result.

We must, however, consider two key differences:

- RAIM-based protection levels rely on more stringent assumptions, e.g. Gaussianity with knowledge of the covariance matrix or absence of multiple fault conditions.
- Isotropy-based protection levels adapt to each situation, changing their size to account for measurement quality and the number of satellites, which makes them much more suitable for the forthcoming multi-constellation scenario.

The significant availability improvement made possible by IBPL appears when the number of satellites used for navigation is big, as with the combined use of two or more constellations (e.g., GPS + GLONASS + Galileo). Starting with the same real-data set used in Fig-

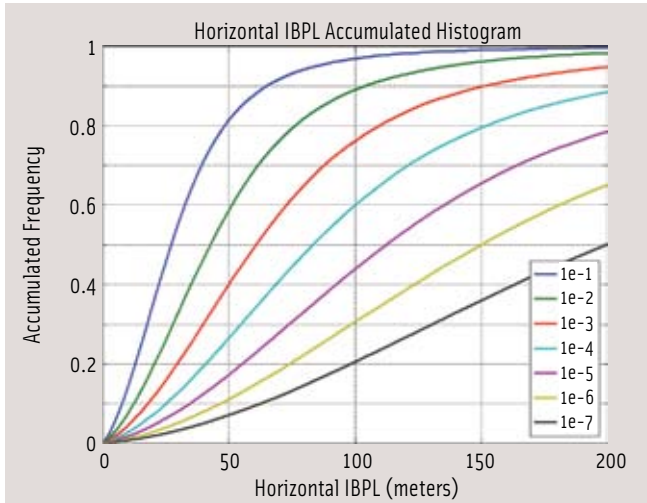


FIGURE 3 IBPL availability in deep urban canyon, GPS + GLONASS/Galileo (extrapolation)

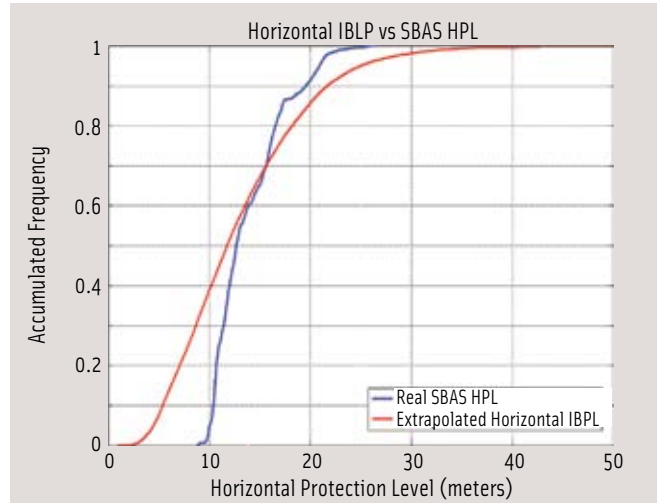


FIGURE 4 Extrapolated horizontal IBPL vs. horizontal SBAS PL

ure 1, we have extrapolated the IBPL behavior with a second constellation (which could be considered to be either GLONASS or Galileo). IBPL extrapolation is made by assuming twice the number of satellites as with only GPS.

Note that the dilution of precision is kept the same as in the GPS-only case, because the second constellation is not simulated but only a doubled number of satellites assumed for the computation of the ICR. (More details about the extrapolation technique will be discussed in the following section.) The results are plotted in **Figure 2**, in which the scale of the horizontal axis has been reduced with respect to Figure 1 for clarity.

The improvement in performance using two constellations is clear when compared with GPS alone represented by Figure 1. Performance is also comparable to current SBAS protection levels. (One should expect improvements of SBAS protection levels associated with a multi-constellation scenario to be caused mainly by a decrease in the DOP, which would also imply an improvement of IBPL with respect to the ones shown here.)

Recall that Figures 1 and 2 correspond to a clear sky environment. IBPL size in other, more aggressive scenarios, such as an urban environment, would increase due to:

- larger measurement residuals caused by larger measurement errors,

because of local effects such as multipath (especially NLoS multipath)

- decreased satellite visibility caused by obstacles (e.g., buildings) that partially occlude the sky view.

**Figure 3** shows an example of IBPL multi-constellation performance in an urban canyon, which is an extrapolation based on a real GPS data set (with 46,881 samples) obtained with a car driving through Salamanca quarter in Madrid. The extrapolation method is the same one used for the open-sky example (Figure 2).

Since the size of IBPL depends linearly on the size of the residuals, and this in turn depends linearly on the size of the errors, all results presented herein would be substantially improved with the accuracy increase that is expected from the evolution of GPS and GLONASS systems, as well as from the future Galileo.

### Asymptotic Convergence of IBPL to SBAS PL

Another remarkable property of the IBPL concept is its convergence to the definition of PL currently used in SBAS (see Annex J of RTCA/DO-229D cited in the Additional Resources section near the end of this article). Roughly speaking, the SBAS definition of PL is:

$$PL_{SBAS} \approx K \cdot \sigma \cdot DoP$$

where  $K$  is the percentile  $1 - \alpha$  of the

centered chi distribution. If the hypotheses assumed in RTCA/DO-229D held (namely, centered Gaussianity with known standard deviation  $\sigma$ ), then the size of the residual vector of the least squares position solution would satisfy:

$$\|r\| \approx \sigma \cdot \sqrt{N-4}$$

On the other hand, the isotropy-based PL is:

$$PL = k \cdot \|r\| \cdot DOP \approx k \cdot \sigma \cdot \sqrt{N-4} \cdot DoP$$

It can be shown by means of Lambert's  $W$ -function that:

$$k \cdot \sqrt{N-4} \xrightarrow{N \rightarrow \infty} K$$

This proves that the IBPL concept converges to the SBAS PL concept when the number of measurements grows.

As an illustration of the preceding theoretical discussion, the extrapolated IBPL curve for  $1 \cdot 10^{-7}$  confidence level (from Figure 2) has been compared with the corresponding SBAS protection level curve. The results are presented in **Figure 4**, which shows, along with the extrapolated IBPL histogram, the corresponding SBAS protection level histogram.

Both curves correspond to the same data set as that used for integrity validation in the earlier section on validating IBPL integrity (i.e., real GPS measurements collected at IGS station Villafranca). For the SBAS protection levels we used that same data set together with real EGNOS messages broadcast dur-

ing the time interval to which the data set corresponds; so, both curves are fully comparable. Note, however, that this is an example based on a particular data set and intended only to illustrate the preceding theoretical discussion; other real-life examples could lead to slightly different results.

Because the IBPL extrapolation assumes twice the number of satellites as with only GPS, it takes at each measurement epoch the ICR that would correspond to twice the number of measurements used for position computation, but leaves the DOP untouched. We have to take into account the fact that using more measurements tends to increase the size of the residual vector. Assuming that the size of the residual vector statistically depends on the number  $N$  of measurements according to the factor  $\sqrt{N-4}$ , and that the noise levels of both GPS and Galileo measurements are the same, the residual vector size—increase factor that results from using  $2N$  measurements (instead of  $N$ ) is:

$$\frac{\sqrt{2N-4}}{\sqrt{N-4}}$$

Of course, this has to be understood as a mere approximation that relies on several assumptions. However, the extrapolated IBPL values that result should not differ too much from the ones that will be obtained with an additional GNSS constellation. Even better results would be expected with the combined use of GPS, Galileo, and GLONASS.

### About the Isotropy Assumption

Once the isotropy assumption has been accepted, the level of integrity achieved with the IBPL concept can be proven mathematically, and is therefore incontrovertible. The only controvertible point of the method is the isotropy assumption itself, or, more precisely, the extent to which this assumption represents the real world.

The first thing to notice is that isotropy is a condition on the behavior of a vector (the vector comprised by the individual errors of the different measurements) that lies in the measure-

ment space. Measurement space is a vector space whose dimension equals the number of measurements used in the computation of a navigation solution and must not be confused with the geometric three-dimensional space that contains the position we want to estimate (nor with the four dimensional space associated with the 3-D position and the clock).

Hence, the isotropy assumption has no relation with satellite line-of-sight geometry (at least not a direct one, though there are some subtleties about this idea that we will discuss later on). The pointing direction of the error vector depends only on the values of the different measurement errors, regardless of the geometric configuration of their lines of sight. So, we can imagine two completely different geometric configurations of the same set of satellites, but if each satellite's measurement error was

the same in both configurations, then the corresponding measurement error vectors would also coincide, both thus pointing in the same direction within the measurement space.

Isotropy means that the error vector has no privileged directions in the measurement space toward which to point. One could argue that the coordinate axes of the space are in fact privileged directions, as each one is used to represent the measurement error of one individual satellite. So, it may seem that a measurement error in a particular satellite would make the measurement error vector to align somewhat with the corresponding axis. However, measurement errors do not come alone: each measurement has its own, and the key point is how they combine to form the measurement error vector. Usually, errors combine randomly to produce an error vector that can point randomly in any direction.

Let us consider for a moment the classic assumption that measurement errors distribute normally, with null mean and some known variance, com-

mon to all satellites. The multivariate statistical distribution of all errors (that is, the distribution of the measurement error vector) is then isotropic. To visualize this, just observe that the associated 1-sigma hyper-ellipsoid is actually a hyper-sphere (and this is a good example to remark the independence of isotropy with respect to line-of-sight geometry).

Isotropy even holds when we allow different variances for different satellites (after the normalization process that transforms the weighted least-squares problem back into an ordinary least-squares one). Therefore, isotropy is, at the very least, a less restrictive assumption than the usual Gaussian statistical models assumed in most RAIM techniques.

However, the authors believe that isotropy is more than just a less stringent assumption. It is instead actually

### The IBPL method does not require, in principle, any ground monitoring [...] thus simplifying ground segment design.

representative of the real world, because even when the axes of the measurement space could be privileged lines, they are also free to point to any direction in the measurement space themselves.

To understand this point, let us recall that the important thing about the heading direction of the error vector is that it determines the relation between the two orthogonal components,  $H \cdot \delta$  and  $r$ , of the error vector. So, as the image of  $H$  (as a vector subspace of the measurement space) changes its orientation with respect to the axes of the measurement space, the axes change their pointing directions relative to the image of  $H$ . Therefore, the relation between  $H \cdot \delta$  and  $r$  changes even if the error vector is bound to a particular axis.

In the preceding discussion, however, we have made use of the change of orientation of the image of  $H$  within the measurement space, and that is directly linked to variations of the satellite line-of-sight geometry. In this sense, the isotropy assumption is related to satellite geometry.

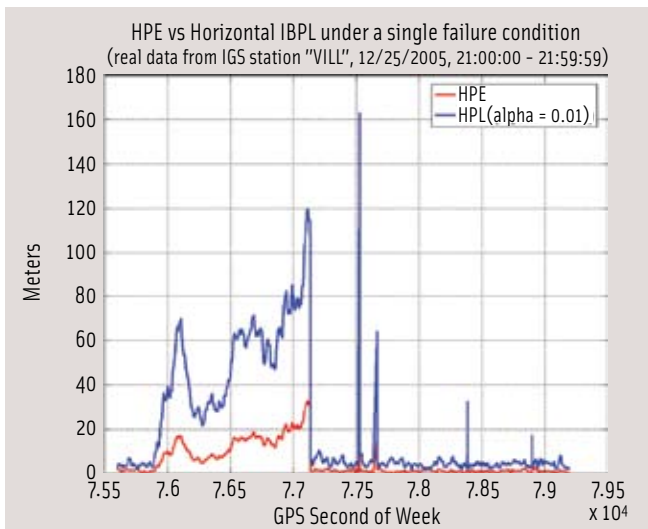


FIGURE 5 Horizontal IBPL vs. horizontal position error under a single failure

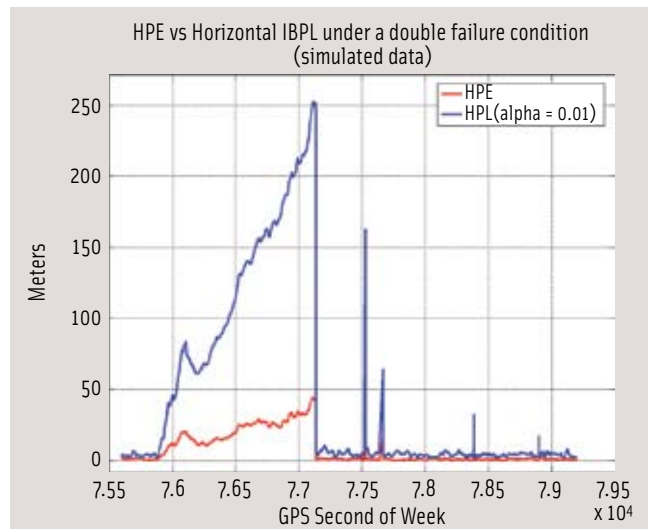


FIGURE 6 Horizontal IBPL vs. horizontal position error during a double failure

Another subtle reason suggests why satellite geometry can indirectly affect the isotropy hypothesis: although we have remarked that the pointing direction of the measurement error vector is independent of the satellite geometry (but is determined only by the values of the measurement errors), this independence would be lost if some correlation existed between satellite geometry and measurement errors (e.g., larger errors at lower elevations). However, this problem can be overcome by modeling such a geometric correlation of errors by means of weighting strategies like those used in all other integrity provision schemes (either autonomous or augmentation-based).

What we claim is that the isotropy assumption is a solid one when we consider the overall statistics, involving all possible geometries and letting time run forever. That is, if we are given a sufficiently large set of samples from real life, each of them taken randomly (randomly also in what concerns satellite geometry), the MI rate obtained from such a sample with the IBPL would be consistent with the theoretical confidence level used to compute said IBPL.

It is a matter of fact that civil aviation requirements do not allow us to average satellite geometries when evaluating integrity performance; so, in order to satisfy these requirements we would

need isotropy to hold for each single geometry. That is, we would have to show that, for each possible satellite geometry, the real-life statistical behavior of ranging errors associated to that particular geometry is isotropic. That is not only difficult to prove, but possibly false.

The authors are aware that this is a potential issue for the application of the IBPL to civil aviation, and further work is being carried out in order to overcome this problem. We think it worthwhile to remark, however, that the issue of averaging geometries is less critical for liability critical applications, in which multipath is the predominant error source and the motion relative to the obstacles causes satellite geometry to change very quickly and quite randomly, even for a fixed route.

We have centered our discussion on the isotropy assumption on the faulty case, because in fault-free conditions it does not seem reasonable to think that the axes of the measurement space are privileged directions (at least, it is clear that faulty conditions are a much bigger challenge for the isotropy assumption).

To illustrate this discussion, we will include an example of IBPL response to a real-life fault condition. The failure took place December 25, 2005, when the on-board clock of GPS satellite PRN 25 started drifting anomalously at 21:04 (GPS time). At 21:25 the satellite was first

flagged as unhealthy in its broadcast navigation message, and by that time, the satellite's clock had drifted about 100 meters away from the value reported in its broadcast navigation message, causing large position errors for many users.

We have used RINEX data from IGS station at Villafranca del Castillo (Spain) in order to test the reaction of the IBPL to such an event. The resulting horizontal position error (in red) and IBPL (in blue) are plotted over time (from 21:00:00 to 21:59:59) in **Figure 5**.

Observe that we have depicted IBPL at  $1-10^{-2}$  confidence level, since it is closer in size to the position error than at higher confidence levels and therefore makes the picture clearer. In particular, this treatment makes it easy to see that the IBPL evolution mimics that of the position error, keeping it properly bounded at any time during the fault condition.

Because we are claiming the ability of IBPL to handle multiple fault conditions as well, we have tried to find a real-world example. However, even though we know that some of them exist, we did not manage to find any RINEX files that reflect such multiple (even double) fault conditions. So, we decided to simulate our own, taking advantage of the preceding single fault example.

For that purpose we manipulated December 25, 2005, incident's RINEX

file to include a clock drift for PRN 24 similar to that of PRN 25 originally present in the file. The results are depicted in **Figure 6**. As in the single failure case, IBPL is always bounding position error during the period of satellite failures.

## Conclusions

The isotropy-based protection level concept arose as the result of investigations concerning GNSS liability critical applications, in particular in urban environments. The authors found, however, that this notion also shows a great availability performance in open-sky environments and could therefore become a major breakthrough in open-sky SoL applications such as civil aviation. Isotropy-based protection levels are completely autonomous, are easily computable in real time, and rely on a single, quite verisimilar and verifiable hypothesis.

Unlike other approaches for integrity being defined as part of the GEAS initiative, the IBPL method does not require, in principle, any ground monitoring, though detection and exclusion of faulty satellites by the ground segment would help guarantee isotropy, leaving the protection level computation to the user — through the IBPL — and thus simplifying ground segment design.

IBPL's sensitivity to the number of satellites becomes a clear advantage in open sky. With currently no more than 10 satellites in view on average (GPS only) and 20 or even more when considering either GLONASS or the future European Galileo system, this PL concept will predictably yield great performances, with smaller protection levels than those achieved nowadays by existing SBASs such as the U.S. Federal Aviation Wide Area Augmentation System or the European Geostationary Navigation Overlay Service.

## Manufacturers

Open sky real data have been downloaded through the Internet from the IGS data server in the form of observation and navigation RINEX files recorded at the IGS station at Villafranca del

Castillo (Spain), which operates an Ashtech Z-XII3 receiver. Urban canyon data were collected by the authors in Madrid (Spain) by means of a SiRFstar II receiver, **SiRF Technology**, San Jose, California, USA. Data processing algorithms were developed by GMV Aerospace and Defence S.A. using Matlab from **The Mathworks, Inc.**, Natick, Massachusetts, USA.

## Additional Resources

[1] Cosmen-Schortmann, J., and M. Martínez-Olagüe, M. Toledo-López, and M. Azaola-Saenz, "Integrity in Urban and Road Environments and Its Use in Liability Critical Applications," Proceedings of the Position Location and Navigation Symposium (PLANS) 2008, Monterey, California, May 6–8, 2008

[2] *GNSS Evolutionary Architecture Study, Phase I - Panel Report*, February, 2008, available on-line at [http://www.faa.gov/about/office\\_org/headquarters\\_offices/ato/service\\_units/techops/navservices/gnss/library/documents/media/GEAS\\_PhaseI\\_report\\_FINAL\\_15Feb08.pdf](http://www.faa.gov/about/office_org/headquarters_offices/ato/service_units/techops/navservices/gnss/library/documents/media/GEAS_PhaseI_report_FINAL_15Feb08.pdf)

[3] RTCA Inc., RTCA/DO-229D, "Minimum Operational Performance Standards for Global Positioning System/Wide Area Augmentation System Airborne Equipment," 2006

## Authors



**Miguel Azaola-Saenz** has an M.S. in mathematics from the University Complutense of Madrid and a Ph.D. in geometry and topology from the University of Cantabria (at Santander), Spain. He has worked at GMV since 2001 as an engineer in several GNSS projects related to both the ground and the user segments. Since 2005 he has been involved in user segment R&D activities at engineering and management levels.



**Joaquín Cosmen-Schortmann** has an M.S. in aerospace engineering from the Polytechnic University of Madrid. He has worked at GMV since 1986. In 1995 he became responsible for GNSS business in GMV with a very active role in the development of EGNOS and Galileo systems. He is currently the CEO Advisor for GNSS matters. 



see what's new  
online  
insidegnss.com